Oxidation state of a buried interface: Near-edge x-ray fine structure of a crystal truncation rod

E. D. Specht and F. J. Walker*
Metals and Ceramics Division, Oak Ridge National Laboratory, Oak Ridge, Tennessee 37831-6118
(Received 16 December 1992)

We observe that the crystal-truncation-rod (CTR) diffraction from the Al_2O_3 substrate of an $Al_2O_3/Cr_2O_3(001)$ interface has fine structure when the x-ray energy is tuned through the Cr K absorption edge. This fine structure is attributed to interference between scattering from the substrate and Cr atoms at the interface, which are coherent with the substrate. Comparisons with x-ray-absorption spectra of standard samples demonstrate that the Cr at the interface is predominantly in the Cr^{3+} oxidation state. We demonstrate how the near-edge energy dependence of the CTR diffracted intensity may be used to deduce the amplitude *and phase* of the interface scattering. This phase information is used in conjunction with reciprocal-lattice-vector-dependent measurements of diffracted power due to CTR's to deduce the structure of the Cr_2O_3/Al_2O_3 interface. While the local atomic coordination at the interface is the same as that of Al_2O_3 and Cr_2O_3, there is a stacking fault at the interface covering half of the interface area.

I. INTRODUCTION

In recent years, x-ray diffraction (XRD) has been applied to the study of interfaces. While most work has been concerned with surfaces,[1] the penetrating nature of x rays makes them well suited to the study of buried interfaces.[2–7] When the periodicity of a crystalline substrate is truncated at an interface but is extended in the plane of the interface, rods of diffraction called crystal truncation rods (CTR's) are observed with the in-plane periodicity of the substrate.[8,9] An overlayer which has a periodicity different from the substrate (or no periodicity at all) will produce no scattering along the substrate CTR's. Overlayer atoms close to the interface will undergo displacements with the periodicity of the substrate. Diffraction from these displaced atoms will interfere with CTR diffraction, so measurements of power diffracted along the CTR's can be used to locate these atoms. Fontes *et al.*[10] treat the case of an incommensurate modulated overlayer, showing that the overlayer affects substrate CTR intensities to the extent that the overlayer is modulated. Reiter and Moss[11] show the same for a liquid overlayer. Substrate CTR intensities have been analyzed to locate commensurate,[3] incommensurate,[5,10] liquid,[11] and amorphous[2] overlayers.

While Bragg diffraction gives the long-range structure of a crystal, x-ray-absorption spectroscopy (XAS) is used to determine the oxidation state, bonding, and local environment of an element.[12] The absorption of x rays by a material increases abruptly as the x-ray energy is increased through an atomic absorption edge of any its constituent elements; the details of the absorption process are affected both by the electronic state of the excited element (reflected primarily in near-edge structure) and by the positions of neighboring atoms, which give rise to characteristic oscillations called the extended x-ray-absorption fine structure (EXAFS). While XAS of surfaces has been conducted by limiting the penetration depth of x rays,[12] the technique has thus far not been applied to buried interfaces.

In this paper, we demonstrate how measurements of the diffraction from an interface may be used to extend the methods of XAS to a buried interface. The energy dependence of diffracted power is measured and related to the absorption cross section. The elastic scattering of an atom to x rays by an atom depends on a complex atomic scattering factor[13]

$$f=f_0(\mathbf{q})+f'(E)+if''(E) \tag{1}$$

which depends both on momentum transfer $\mathbf{q}$ and energy E. Because the scattering factor depends strongly on energy only near atomic absorption edges, the energy-dependent portion is referred to as anomalous scattering. The linear absorption coefficient

$$\mu=2n\sigma_T^{1/2}\lambda f'' \tag{2}$$

depends only on the imaginary part of the scattering factor, while the structure factor

$$F=\sum_i f_i \exp(i\mathbf{q}\cdot\mathbf{r}_i) \tag{3}$$

depends on both the real and imaginary parts, and of course the crystal structure. $\sigma_T=7.94\times10^{-26}$ cm^2 is the Thomson cross section, n is the number density of atoms, λ is the x-ray wavelength, and the $\mathbf{r}_i$ are atomic positions. The sum runs over all atoms in a unit cell. The scattering factor for a CTR is calculated using a two-dimensional unit cell which reflects only the extended periodicity in the plane of the interface; the sum (now semi-infinite) runs over all atoms in the direction normal to the interface.[1] Because the two energy-dependent terms f' and f'' of the scattering factor in Eq. (1) are related by the Kramers-Kronig transform[14,15]

$$f'(E_0)=\frac{2}{\pi}\mathbf{P}\int_0^\infty \frac{Ef''(E)}{E_0^2-E^2}dE\ , \tag{4}$$

 ©1993 The American Physical Society

(P denotes the principal part of the integral), we can (at least in principle) gain the same information from measurements of the energy dependence of the structure factor as from measurements of the energy dependence of absorption. Stragier *et al.*,[16] for example, have shown that the coordination of copper can be measured from extended fine structure in Bragg diffraction as well as from EXAFS.[16] By measuring the near-edge structure in the CTR diffraction, spectroscopic measurements can be made which are sensitive to the chemical state at a buried interface.

The modification of materials properties near interfaces is the basis of much of our technology, from the oxide layers which render metallic surfaces nonreactive to the depletion layers which lead to rectification in semiconductor junctions. Diffraction from a CTR contains information concerning just those overlayer atoms which are displaced by a substrate. Using this diffraction technique, we can single out the overlayer material which is strongly affected by the substrate.

This paper presents an analysis of diffraction from the interface between an $Al_2O_3(100)$ substrate and a Cr_2O_3 film near the Cr K absorption edge. Section II describes the measurement of the energy dependence of $|F|^2$ for a CTR. Section III describes measurements of f' and f'' for Cr metal and Cr^{+3} standards. In Sec. IV, the energy dependence of the CTR is compared with those of the standards to determine the oxidation state of Cr at the interface, and in Sec. V the energy dependence of the CTR diffraction is used to determine the phase of the scattering from Cr and thus the structure of the interface. Section VI presents the interpretation of the results.

II. MEASUREMENT OF $|F|^2$

Cr_2O_3/Al_2O_3 was chosen as a test system because the film grows with good epitaxy and the absorption spectra of the oxidation states of Cr are readily distinguished.[17,18] Cr was deposited from an effusion source onto a (001) α-Al_2O_3 (sapphire) substrate heated to ~ 1000 K in a 10^5-Torr O_2 atmosphere, using the molecular-beam-epitaxy apparatus described by McKee, List, and Walker.[19] The film was grown to a 142-mm thickness. XRD and reflection high-energy electron diffraction (RHEED) confirmed that the film grew with the Cr_2O_3 structure and indicated two epitaxies, both with Cr_2O_3 (00.1) parallel to Al_2O_3 (00.1). Equal fractions grew with Cr_2O_3 [10.0] parallel to Al_2O_3 [10.0] (parallel epitaxy) and to Al_2O_3 [11.0] (rotated 60° about [00.1]).

CTR fine-structure measurements were used to determine the oxidation state of Cr at the interface. XRD was conducted at beamline X-14 of the National Synchrotron Light Source.[20] Two parallel Si(111) crystals were used to scan the x-ray energy E through the Cr K edge at 6.00 keV. The sample was mounted under a Be dome in a He atmosphere on a four-circle diffractometer. The diffracted power due to Al_2O_3 CTR's was measured at each energy as follows. Slits were used to obtain a small (0.6×0.6 mm^2) incident beam. A N_2-filled ion chamber immediately downstream from the incident-beam slits was used to monitor incident power. Diffracted x rays entered a scintillation detector through a large (5×5 mm^2) receiving slit at a distance $R=595$ mm downstream from the sample. The combination of small incident and large receiving slits insures that all diffracted x rays are collected. We verified this by scanning the diffracted beam through a narrow receiving slit. By scanning 2θ (2θ, ω, ϕ, and χ are four-circle diffractometer angles[21]), we find the width of the diffracted beam to be $R\Delta 2\theta=2.7$ mm full width at half maximum (FWHM) in the in-plane direction; by scanning χ, we find the width to be $2R\sin\theta\Delta\chi=1.9$ mm in the out-of-plane direction.[22]

To deduce the structure factor $|F|$ from the total diffracted power due to the CTR, the sample is rotated to discriminate between CTR diffraction and background by scanning ϕ and fitting the rocking curve to the sum of a Pearson-7 function[23] and a constant. The maximum of the Pearson-7 function is the diffracted power, while the background is dominated by Cr fluorescence from the film.

We find $|F|^2$ in electron units using the relation[22]

$$|F|^2=\frac{P_{\rm CTR}}{\sigma_T P_0}\left[\frac{a_0\sin\theta\sin\chi}{\lambda}\right]^2\exp\left[\frac{2\mu T}{\sin\theta\sin\chi}\right], \tag{5}$$

where a_0 is the area of a two-dimensional unit cell. The method for measuring the linear x-ray-absorption coefficient μ is described in Sec. III. $T=142$ nm is the film thickness, deduced from the period of the oscillations in the low-angle x-ray reflectivity.[24] P_0 and $P_{\rm CTR}$ are the incident and diffracted power. P_0 is measured at each energy (including absorption for air and windows), using a p-i-n diode to accommodate count rates of $\sim 10^{10}$ s^{-1}. The response of the scintillation counter and the p-i-n diode are then compared at each energy, at a lower count rate, by measuring a Cr_2O_3 film integrated (11.3) Bragg reflection with each detector. Since this calibration depends on the electrometer linearity over a power range of 10^6 from the CTR diffraction to the direct beam, we include one arbitrary overall scale factor for $|F|^2$. The absolute magnitudes in electron units are determined by varying this scale factor to fit calculated values for a model structure, as described in Sec. V.

The reciprocal-lattice vector (RLV) at which $|F|^2$ is measured must be chosen carefully to obtain high sensitivity to the energy dependence of the Cr scattering. The structure factor may be written as

$$F=A_{\rm substrate}e^{i\phi_{\rm substrate}}+S_{\rm Cr}e^{i\phi_{\rm Cr}}(f_0+f'+if''), \tag{6}$$

where $A_{\rm substrate}$ is the modulus of the structure factor for the substrate as well as O atoms in the film and $S_{\rm Cr}$ is the structure factor for Cr atoms. Atomic scattering factors are included implicitly in $A_{\rm substrate}$, but not in $S_{\rm Cr}$. The diffracted power is proportional to

$$\langle|F|^2\rangle=\langle I_0\rangle+\langle I'\rangle f'+\langle I''\rangle f''+\langle I_2\rangle, \tag{7}$$

where

$$I_0 = A^2_{\text{substrate}} + (S_{\text{Cr}} f_0)^2 + 2A_{\text{substrate}} S_{\text{Cr}} f_0 \cos(\phi_{\text{Cr}} - \phi_{\text{substrate}}) ,$$
$$I' = 2A_{\text{substrate}} S_{\text{Cr}} \cos(\phi_{\text{Cr}} - \phi_{\text{substrate}}) + 2S^2_{\text{Cr}} f_0 , \quad (8)$$
$$I'' = -2A_{\text{substrate}} S_{\text{Cr}} \sin(\phi_{\text{Cr}} - \phi_{\text{substrate}}) ,$$
$$I_2 = S^2_{\text{Cr}} (f'^2 + f''^2) ,$$

and $\langle\ \rangle$ denotes an average over thermal fluctuations and over different interface structures (as we discuss in Sec. V, the symmetry of the substrate leads to two symmetry-related interface structures). Close to the Bragg peaks, $A_{\text{substrate}} \gg S_{\text{Cr}}$, so the coefficients I' and I'' of the energy-dependent terms are *relatively* too small to measure: $|F|^2$ would have to be measured with high precision to detect its energy dependence. Far from the Bragg peaks, $A_{\text{substrate}}$ is small, so I' and I'' are *absolutely* too small to measure. Measurements far from the Bragg peaks require higher flux x-ray sources to detect the weaker scattering; even so, the CTR signal will be small relative to the diffuse background, especially for substrates such as Al_2O_3, where the x-ray penetration depth is large. The energy dependence is best observed at an intermediate point along the CTR, where S_{Cr} is as large as possible.

The relative phase ϕ_{Cr}-$\phi_{\text{substrate}}$ is also a factor in how well the energy dependence of $|F|^2$ can be measured. Equations (7) and (8) show that this phase determines whether the scattering varies as f' or as f''. Because absorption by the film varies as f'', we choose (as described below) a RLV where the scattering is observed to vary as f', to avoid the possibility of mistaking an improper absorption correction for anomalous scattering from the interface. The maximum linear x-ray-absorption coefficient for Cr_2O_3 above the Cr K edge (measured as described in Sec. III) is 2.6×10^{-4} nm^{-1}; for scattering at $\sin\theta \sin\chi = 0.25$, absorption from the overlayer would be a negligible 1% for a thickness of 4.8 nm. Rather than use such a thin film, we chose to use a thicker (142-nm) film to protect the interface from contamination. For this reason, we make a careful measurement of and correction for absorption.

A survey of reciprocal space was made to determine the optimum RLV for the measurement of anomalous scattering. The in-plane lattice constant of Cr_2O_3 is 4.1% greater than that of Al_2O_3; this misfit leads to displacements of interface atoms from ideal registry with the substrate. These displacements reduce the intensity of interface scattering to CTR's with high in-plane momentum transfer.[5] Just as for thermal motion of atoms, a mean-square displacement $\langle u^2 \rangle$ in the direction of the momentum transfer $\mathbf{q}$ reduces diffracted power by $\exp(-q^2\langle u^2\rangle)$.[25] We therefore restricted the search to the low-order CTR's, with RLV's of $(10.l)$, $(0.1l)$, and $(11.l)$. The diffracted power was relatively low along $(10.l)$ and $(01.l)$. This is a result of the Al_2O_3 crystal structure, which we will discuss in more detail in Sec. V. The Al_2O_3 lattice is hexagonal with $a = 0.4763$ nm. If small distortions are neglected, both the Al and O atoms each lie on a hexagonal sublattice with periodicity $a = 0.4763/\sqrt{3}$ nm. Thus $(11.l)$ peaks are strong fundamental peaks, while $(10.l)$ and $(01.l)$ peaks are weaker superstructure peaks which are present only due to distortions in the O sublattice and ordered vacancies in the Al sublattice. The diffracted power at $(11.l)$ was measured for a series of l with $E = 5.94$ and 5.98 keV at each RLV. Only f' changes significantly between 5.94 and 5.98 keV (just below the Cr K edge), so the ratio of diffracted power $P(5.98)/P(5.94)$ (Fig. 1) yields the magnitude of I'/I_0; $P(5.98)/P(5.94)$ is proportional to $1 - I'/I_0$. The error bars in Fig. 1 are the uncertainty due to counting statistics. As shown in Fig. 1, this ratio will be indistinguishable from 1 if no Cr atoms are coherent with the substrate. The RLV with the best combination of large I'/I_0 and high count rate was found to be (1,1,.,3.25). Figure 2 illustrates the variation in $|F|^2$ at this RLV as the x-ray energy is tuned through the Cr absorption edge.

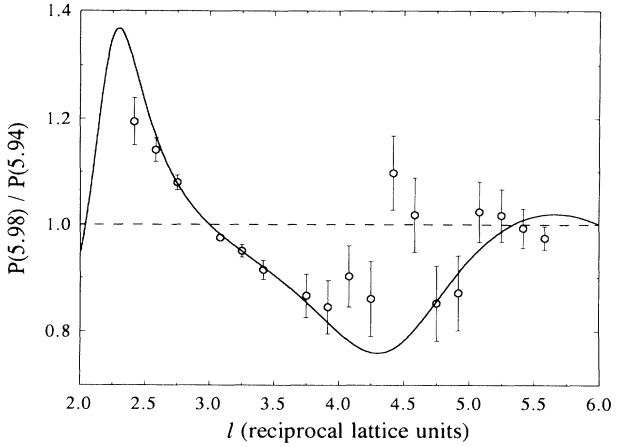

FIG. 1. The ratio of diffracted power due to the CTR at $(11.l)$ for $E = 5.98$ and 5.94 keV. The circles are observed values; the solid line is calculated from the structural model described in Fig. 5 and Table I, and the dashed line is calculated for truncated Al_2O_3 with no coherent Cr atoms.

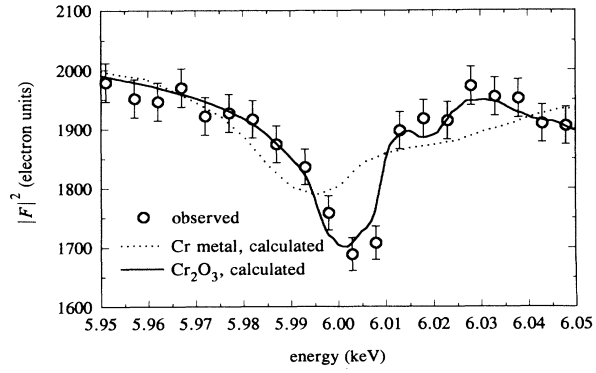

FIG. 2. The energy dependence of the CTR diffraction at (1,1.,3.25). The solid line is a calculated fit using experimental values of f' and f'' from either Cr metal (dotted line) or Cr^{+3} (solid line).

III. MEASUREMENT OF ANOMALOUS SCATTERING FACTORS f' and f''

The energy dependence of $|F|^2$ for the Al_2O_3 CTR's is compared with experimentally determined values of the anomalous scattering factors for Cr^{+3} and Cr metal. In each case, we measure f'' and compute f' with the Kramers-Kronig transform [Eq. (4)]. f'' for Cr metal is computed from the measured K-edge absorption of a Cr film, while f'' for Cr^{+3} is computed independently from measurements of Cr K-edge absorption and fluorescence of a Cr_2O_3 film. The absorption measurements are based on the attenuation of the Al_2O_3 (11.3) Bragg peak by a Cr_2O_3 overlayer. The (11.3) integrated reflection is found by integrating a ω rocking curve, using a p-i-n diode as a detector. The linear absorption coefficient is

$$\mu=\frac{\sin\theta\sin\chi}{2T}\ln(DE_{\rm calc}/E_{\rm obs}) , \tag{9}$$

where the calculated integrated reflection is[26]

$$E_{\rm calc}=P_0\left[\frac{8\sigma_T^{1/2}N}{3\pi\dot{\omega}}\right]\frac{|F|\lambda^2}{\sin2\theta} . \tag{10}$$

N is the number density of unit cells and $\dot{\omega}$ is the angular velocity of the scan. The formula for a perfect crystal with no absorption is used because the Al_2O_3 (11.3) extinction depth of 43 nm is much less than the Al_2O_3 absorption depth of 3.3×10^4 nm. F is determined from the Al_2O_3 structure[27] and the atomic form factors for Al^{+3} and O^-,[28] which include anomalous scattering factors.[29] The relative magnitude of $E_{\rm obs}$, measured as a function of energy, is related to the absolute magnitude by the constant D in Eq. (9), which is determined from the linear absorption coefficient just below the edge given by McMaster *et al.*,[30] and the lattice constants of Cr_2O_3 from Saalfeld.[31] f'' for Cr metal is computed in a similar manner from the measured x-ray absorption by a 115-nm film of Cr metal on Al_2O_3.

Because any shifts in the direction of the x-ray beam incident on the monochromator will shift the energy selected by the monochromator, we calibrate the energy scale using data acquired simultaneously with the diffraction data of Fig. 2. f'' is computed from the intensity of Cr $K_{\alpha,\beta}$ fluorescence from the Cr_2O_3 film, which appears as a background to the CTR diffraction. The intensity of the fluorescence is[32]

$$Y=\frac{C\mu_K}{\mu_T+\mu_F}\left[1-\exp\left[-T\frac{\mu_T+\mu_F}{\sin\theta\sin\chi}\right]\right] , \tag{11}$$

where μ_K is the linear absorption coefficient due to the Cr K shell photoabsorption, μ_T is the total linear absorption coefficient of Cr_2O_3 (both for the incident x rays), μ_F is the total linear absorption coefficient for the Cr K fluorescence, T is the film thickness, and C is a constant which depends on incident x-ray power. We take μ_T and μ_F from McMaster *et al.*,[30] using for μ_F the absorption coefficient at the Cr K_α energy, and the Cr_2O_3 density from Saalfeld.[31] From the absorption measurement described above for the Cr_2O_3 film's linear absorption coefficient, we know the maximum value of μ_K; we use this value to solve Eq. (11) for C at 6.009 keV, the energy at which Y is maximum. We use this value of C in Eq. (11) to find μ_K and, from Eq. (2), f'' at each energy.

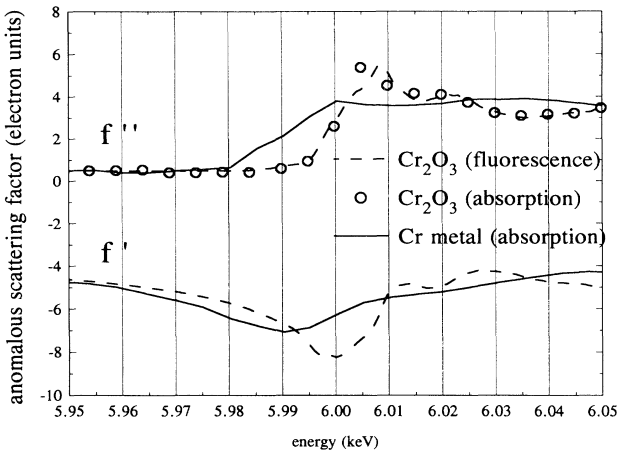

FIG. 3. Anomalous scattering factors for Cr and Cr_2O_3 films computed from absorption and fluorescence measurements.

As shown in Fig. 3, these independent determinations of f'' for Cr_2O_3, one from fluorescence (dashed line) and one from absorption (circles), are in good agreement. Both determinations agree qualitatively with the data taken from bulk Cr_2O_3 powder.[17] We expect the thin-film data to be quantitatively more accurate because the film is of very uniform thickness. The bulk oxide powder is known to be stoichiometric Cr_2O_3, so the qualitative agreement confirms that the film, although grown under low oxygen pressure, is stoichiometric as well. In further analysis we use the fluorescence data, which includes less noise. The energy scale of each spectrum has been set so the absorption edge (the lowest energy where f'' reaches half its maximum value) falls at the values determined by Grunes:[17] 5.9890 keV for Cr and 5.9998 keV for Cr_2O_3.

The Kramers-Kronig transform [Eq. (4)] was used to calculate[33] f' from f''. Figure 3 shows these anomalous scattering factors. Because the absorption edge is 10 eV lower in energy for the metal than for the oxide, we can use the energy dependence of the interface diffraction to determine the oxidation state of Cr at the interface.

IV. Cr OXIDATION STATE

We determine the oxidation state of Cr atoms at the interface by comparing the energy spectrum of $|F|^2$ (Fig. 2) with that of the anomalous scattering factors f' and f'' (Fig. 3) for both Cr metal and Cr_2O_3. We fit $|F|^2$ to Eq. (6) with $A_{\rm substrate}$, $S_{\rm Cr}$, and $\phi_{\rm Cr}$-$\phi_{\rm substrate}$ as free parameters. The best fits for the two oxidation states is shown in Fig. 2. The rms error is 3.4% for Cr metal but only 1.2% for Cr_2O_3, roughly the statistical uncertainty of the data, with $S_{\rm Cr}=5.86\times10^{-3}$ $A_{\rm substrate}$, and $\phi_{\rm Cr}$-$\phi_{\rm substrate}=21°$. Thus we conclude that the Cr atoms at the interface which are in phase with the substrate are in the Cr^{+3} oxidation state.

XRD and RHEED confirm that the bulk of the film is Cr_2O_3. From this structural measurement, we infer that in the bulk of the film Cr is in the Cr^{+3} oxidation state. *In situ* RHEED shows the first atomic layers of the film to be disordered. Because of this disorder, the RLV dependence of the diffraction does not contain enough information to determine the structure of the material near the interface; we cannot deduce the oxidation state from the structure. The energy dependence of the diffraction allows us to determine the oxidation state more directly.

We have determined the oxidation state of the Cr atoms which contribute to the CTR diffraction without the need to know the interface structure. We next use the intensity of diffraction along the CTR, and its energy dependence, to determine where these Cr atoms lie with respect to the substrate.

V. INTERFACE STRUCTURE

We infer the interface structure based on a combination of the energy dependence of the diffracted power from the CTR at one RLV, (1,1.,3.25) (Fig. 2), and the RLV dependence at one energy, 5.70 keV (Fig. 4). From the RLV dependence of the diffracted power, we determine the amplitude of F, while from the energy dependence we find the relative phase of F for the substrate and Cr atoms at the interface. We first discuss the structure and symmetry of the substrate, proceed to describe how $|F|^2$ may be calculated for a model interface, and then construct a model which fits both the energy- and CTR-dependent data.

Bulk Al_2O_3 and Cr_2O_3 each consist of a distorted hexagonal close packing of O atoms with octahedrally coordinated Al or Cr in two-thirds of the interstices, as shown in Fig. 5, layers $L1$–$L4$.[27] We designate the O stacking sequence as AB, and the Al/Cr sites as C. O atoms are displaced from close-packing sites within the (001) planes, while Al and Cr layers are buckled in the [001] direction. See Wyckoff[27] for details of atomic displacements from high-symmetry sites and ordering of metal atoms on C sites in the bulk structure. For one of the epitaxies we observe that, in the Cr_2O_3/Al_2O_3 film, the O sublattices of the film and substrate have the same orientation, and for the other they are rotated 60° about [001]. Both these epitaxies are consistent with an O sublattice which preserves close packing locally across the interface, although long-range order must be disrupted by misfit dislocations and other defects. Either epitaxy is consistent both with a locally continuous hexagonal close packing and with an oxygen sublattice containing a stacking fault; e.g., $\cdots ABABCBCB\cdots$.

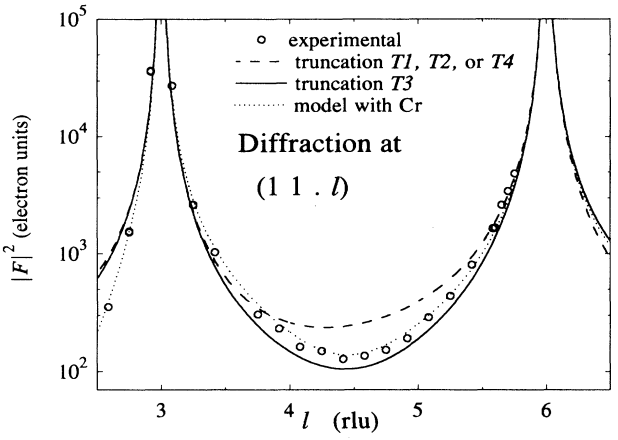

FIG. 4. The diffracted power due to the CTR at (11.l), as measured and as computed for Al_2O_3 truncated by a plane and for the structural model described in Fig. 5 and Table I.

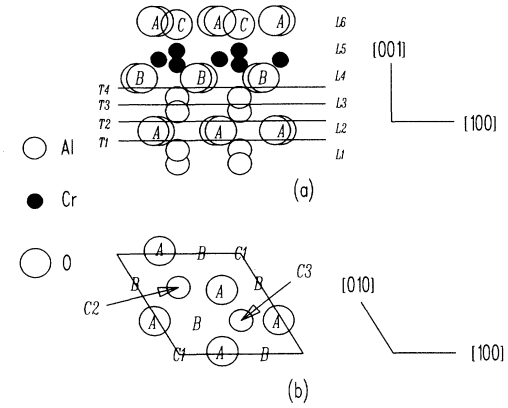

FIG. 5. The model for the structure of the Cr_2O_3/Al_2O_3 interface, as determined from energy- and RLV-dependent diffraction. $T1$–$T4$ denote truncation planes of Al_2O_3 referred to in the text, while $L1$–$L6$ label atomic layers. A, B, $C1$, $C2$, and $C3$ label positions in the (001) plane occupied by close-packed atoms (see Table I for their coordinates). (a) is a [120] projection of the structure, (b) a [001] projection of bulklike Al_2O_3 layers $L1$ and $L2$ only.

While the O sublattice has an approximate sixfold symmetry about [001], the sites occupied by the Al sublattice reduce the symmetry to threefold. We observe equal populations for the two epitaxies, aligned and rotated 60°, which suggests that there are no correlations between the sites occupied by the Al in the substrate and the Cr in the film.

Now consider the scattering from an Al_2O_3 surface. We model the Al_2O_3 as a lattice truncated at a (001) plane. In the kinematic approximation, the diffracted power from a CTR is proportional to $|F(\mathbf{q})|^2$, where[9]

$$F_{\text{substrate}}(\mathbf{q})=\sum_{n=0}^{\infty}\left[\sum_{j=1}^{4} f_{\text{Al}} e^{i\mathbf{q}\cdot\mathbf{r}_{\text{Al}}^{j}}+\sum_{j=1}^{6} f_{\text{O}} e^{i\mathbf{q}\cdot\mathbf{r}_{\text{O}}^{j}}\right] e^{in\mathbf{q}\cdot\mathbf{b}} = \frac{\sum_{j=1}^{4} f_{\text{Al}} e^{i\mathbf{q}\cdot\mathbf{r}_{\text{Al}}^{j}}+\sum_{j=1}^{6} f_{\text{O}} e^{i\mathbf{q}\cdot\mathbf{r}_{\text{O}}^{j}}}{1-e^{i\mathbf{q}\cdot\mathbf{b}}} . \tag{12}$$

The unit cell consists of six O atoms at $\mathbf{r}_{\text{O}}^{1}=(0,0.303,\frac{1}{4})$ and symmetry-related sites and four Al atoms at $\mathbf{r}_{\text{Al}}^{1}=(0,0,0.145)$ and symmetry-related sites. Because the interface is periodic only in the two directions parallel to the interface, we must sum over a third translation $\mathbf{b}=(\frac{1}{3},\frac{2}{3},-\frac{1}{3})$ with a component normal to the interface.

This calculation is complete for a lattice truncated by a plane. For a real surface, we must consider the effect of

interface roughness. The space group for Al_2O_3, $R\bar{3}c$, includes three $c(0,0,\frac{1}{2})$ glide planes; this implies that truncations by, for example, planes $T1$ and $T4$ in Fig. 5 differ only by a translation and reflection of the crystal. For a real crystal, we expect these two symmetry-related variants to occur with equal frequency, separated by surface steps of height $c/6$. Because anomalous scattering will break the inversion symmetry of the scattering process, the symmetry of the diffraction pattern will be the point group of the truncated crystal, rather than the Laue group. Each variant will have point group 3, but the two patterns differ by a reflection about $\{100\}$; we expect to observe their average, which will have point group $3m1$. Because the point group of each variant is a subgroup of the point group of the crystal, the point group of a real truncated crystal will be a supergroup of each variant but a subgroup of the crystal's point group. The average diffracted power at any RLV $(hk.l)$ from a surface containing both variants will be the average of the diffracted power from either variant at $(hk.l)$ and $(\bar{k}\,\bar{h}.l)$.

The intensity of the CTR diffraction reflects interference between the substrate and interface. Because a Patterson map based on CTR intensities is dominated by scattering from the substrate, we cannot directly construct the interface structure from these data. Instead, we locate the interfacial Cr atoms by fitting a calculated structure to the observed diffraction pattern. As may be seen from Fig. 4, the RLV dependence of the scattering is close to that of Al_2O_3 truncated by the $T3$ plane. This suggests an abrupt truncation of the Al_2O_3 lattice, so we take this as the starting point.

The simplest class of models we consider is a truncated Al_2O_3 lattice, with Cr atoms replacing the Al near the surface. We consider all combinations of Cr and Al atoms above and below the topmost layer of O atoms, with both full and partial occupation of all sites. For the $(11.l)$ CTR (the only CTR that we consider), each of the three A sites will scatter with the same phase. Therefore, we may take the three A sites to be equally occupied; it is similar for the B and C sites. In Al_2O_3, Al in fact lies on only two thirds of the C sites; other CTR's (or Bragg peaks) must be measured to observe the effect of this preferential occupation. For each model structure, we calculate $|F|^2$ from Eqs. (6), (7), (8), and (12). We fit the RLV dependence of Fig. 4 with the overall intensity as a free parameter. The statistical weight of each data point is taken to be the inverse of its magnitude; in other words, we minimize the mean-square percentage error. We fit the energy dependence of Fig. 2 by fitting the ratios I'/I_0 and I''/I_0, calculated for the model structure using Eqs. (8), to the ratios determined from the measurements. All models which approximate the measured RLV dependence fail to account for the measured energy dependence, and vice versa. For example, the $T3$ truncation gives one of the best fits to the RLV dependence, as shown in Fig. 4, but even when Cr is substituted for Al, the calculated diffracted power for this model is constant as a function of energy. This is a consequence of the averaging between symmetry-related truncations: while either truncation would produce a substantial energy dependence, the energy variations effectively cancel one another.

We are able to describe both the energy and CTR dependence of the data by considering a more general model. As noted above, when Cr_2O_3 grows on Al_2O_3, equal components of the film are aligned and rotated 60° with respect to the substrate. Because stacking faults are a likely cause of such a misorientation, we consider models in which some atoms are stacked in alternative sites. We consider structures where atomic coordination is minimally disturbed: oxygen atoms are close packed, and Cr and Al atoms lie in octahedral sites. Within these

TABLE I. Structure of the Cr_2O_3/Al_3O_3 interface as determined from anomalous x-ray diffraction, including the top four layers of the Al_2O_3 substrate and the portion of the Cr_2O_3 film which is coherent with the substrate. The stacking index indicates the in-plane coordinates: $A=\{(0,\frac{1}{3}),(\frac{2}{3},\frac{2}{3}),(\frac{1}{3},0)\}, B=\{(\frac{2}{3},0),(0,\frac{2}{3}),(\frac{1}{3},\frac{1}{3})\}, C_1=(0,0), C_2=(\frac{1}{3},\frac{2}{3}), C_3=(\frac{2}{3},\frac{1}{3})\}$; O atoms are displaced 0.03 lattice unit from these sites as in the bulk structure. The out-of-plane coordinate is z. We use $\pm$ to indicate pairs of atoms symmetrically displaced as in bulk Al_2O_3; numbers in parentheses are statistical uncertainties in the last digits of the free parameters.

Layer	Element	Stacking index	z (lattice units)	Density (atoms/0.20 nm^2)
		Al_2O_3 substrate		
$L1$	Al	C_2, C_3	± 0.022	2
$L2$	O	A	$\frac{1}{12}$	3
$L3$	Al	C_3, C_1	$1/6 \pm 0.022$	2
$L4$	O	B	$\frac{1}{4}$	3
		Cr_2O_3 atoms in pseudomorphic sites:		
$L5$	Cr	C_1, C_2	$\frac{1}{3} \pm 0.022 - 0.02(2)$	1.0(5)
$L6$	O	A	$\frac{5}{12} + 0.01(4)$	2.1(14)
		Cr_2O_3 atoms in other sites:		
$L5$	Cr	A	$\frac{1}{3} - 0.03(3)$	0.8(4)
$L6$	O	C_1, C_2, C_3	$\frac{5}{12} + 0.0(2)$	0.9(12)

constraints, we find that a necessary and sufficient condition to fit both the energy and RLV dependence is that the first layer of Cr atoms lies on A sites, which would be empty in the Al_2CO_3 structure, as well as on C sites, which would be occupied. We find the best fit when two layers of Cr_2O_3 are included, with positions and occupations as shown in Fig. 5 and Table I. There are nine free parameters: overall intensity and the heights and occupations of the four Cr_2O_3 atomic sites in layers $L5$ and $L6$.

The dotted line in Fig. 4 shows the fit of this model to the RLV dependence of the scattering; the rms percentage error is 17%. As noted above, these observations are approximately described by a simple truncation of the Al_2O_3 lattice. It is the energy-dependent measurements which demonstrate coherence between Cr atoms and the Al_2O_3 substrate. While more accurate and extensive measurements of the RLV dependence of diffracted power would improve our ability to discriminate between structural models, it is the energy dependence which provides the critical ability to distinguish between Al and Cr atoms. In Fig. 6, we compare the energy dependence predicted by this model to that observed at (1,1.,3.25). The predicted $|F|^2$ (solid line) is less than the observed values (circles) at lower energies, greater at higher energies. This implies that the predicted $|F|^2$ contains a larger component proportional to f''. In the notation of Eqs. (7) and (8), the predicted value of I'' is greater than that observed, due to a difference in the relative phase ϕ_{Cr}-$\phi_{substrate}$ of the Cr scattering. While we can best fit the energy dependence by ϕ_{Cr}-$\phi_{substrate}=21°$ (as in Fig. 2), the model structure gives ϕ_{Cr}-$\phi_{substrate}=-32°$. These deviations between calculated and observed diffraction may be attributed to the simplifying assumption that all atoms lie on high-symmetry sites. If the Al_2O_3 is truncated with no coherent Cr atoms, the energy dependence of the structure factor due to the anomalous scattering of Al and O atoms is negligible, as shown by the dashed line in Fig. 6, calculated for truncation at the $T3$ plane (Fig. 5). Figure 1 compares the data on the change in diffracted power between 5.94 and 5.98 keV with the predictions of this model. The model accounts well for the trends in energy dependence over a wide range of RLV's.

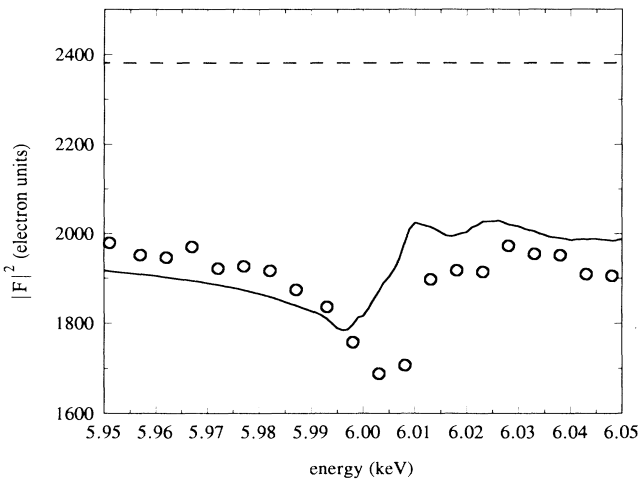

FIG. 6. A comparison of the measured energy dependence of the diffracted power at (1,1.,3.25) (circles) to the energy dependence calculated from the structural model shown in Fig. 5 and Table I (line), and for simple truncation of the Al_2O_3 lattice by the $T3$ plane (Fig. 5).

VI. DISCUSSION

The interface structure presented in Fig. 5 and Table I requires some interpretation. The observations suggest that both A and C sites of layer $L5$ are occupied by Cr atoms. In the bulk Cr_2O_3 structure only one such site is occupied, so we infer that occupation of neighboring A and C sites is energetically unfavorable and that the interface consists of clusters, with only one site occupied in each cluster, as shown in Fig. 7: dotted lines separate Cr atoms occupying A sites in the upper cluster and C sites in the lower cluster. The density of layer $L5$ is, within experimental uncertainty, equal to that of the bulk, indicating that atoms within each cluster are well registered with respect to the substrate.

The structure of this layer may be understood based on growth kinetics. We expect layer $L5$ to nucleate with a cluster of atoms on site C, following the common structure of Al_2O_3 and Cr_2O_3. Due to the 4.1% lattice mismatch, as this cluster grows, atoms at the edge will be pushed off the C sites onto A sites, nucleating a cluster with differing registry. Oxygen atoms in layer $L6$ will fall on the sites which provide octahedral coordination for the Cr atoms: Cr atoms on C sites will be covered with O atoms on A sites, while Cr atoms on A sites will be covered with O atoms on C sites.

The model includes Cr atoms at two sites in registry with Al_2O_3. The C sites of layer $L5$ form part of a layer of Cr_2O_3 growing pseudomorphically on Al_2O_3. The coordination of these atoms is that of bulk Cr_2O_3, consistent with the close agreement between the CTR x-ray fine structure and that of Cr_2O_3. The coordination of

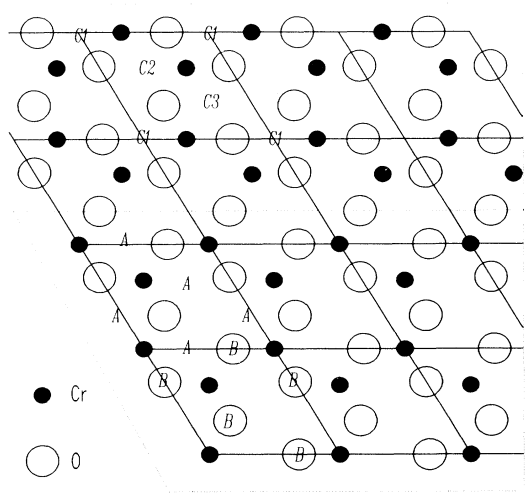

FIG. 7. The [001] projection of layers $L4$ and $L5$ of the model interface, illustrating how clusters of Cr atoms occupy A (upper half) and C sites above a layer of O atoms on B sites.

nonpseudomorphic Cr atoms on the A sites in layer $L5$ is similar to that of bulk Cr_2O_3. As shown in Fig. 7, the nonpseudomorphic A sites in layer $L5$ have the same coordination with respect to the O atoms in layer $L4$ as do the pseudomorphic C sites; in the model structure, O atoms in layer $L6$ provide octahedral coordination to each Cr atom. For these atoms too, the structure is consistent with the bulk Cr_2O_3 fine structure.

The energy-dependent and RLV-dependent measurements are complementary. The energy dependence of the diffraction alone tells us the oxidation state of the Cr, but does not tell us precisely where the Cr is; it is by considering the RLV dependence that we can determine that only one or two layers of Cr are coherent with the substrate and thus contribute to CTR diffraction. Conversely, we would be unable to determine unambiguously the structure of the interface from the RLV-dependent data alone. In the case of a perfect crystal, the structure factors of many Bragg reflections may be measured to resolve structural ambiguities. For an interface which is poorly ordered due to lattice misfit, strong scattering due to the interface occurs only for low-order CTR's, so the range of useful structure factors is limited.[5] Only by using anomalous scattering can we distinguish a heavy atom (e.g., Cr) with a low degree of registry with the substrate from a lighter atom (e.g., Al) with a higher degree of registry.

It is tempting to interpret the oscillations observed in Fig. 2 as EXAFS. In principle, by measuring diffracted power over a wider energy range, one can determine the coordination of atoms. Stragier *et al.* have demonstrated that the coordination of copper may be confirmed from the energy dependence of its diffraction.[16] Our measurements were made with an incident flux of $\sim 10^{10}$ photons/s; several days would be required to conduct an EXAFS measurement at that rate. The stability exhibited in Fig. 2 does not extend to these longer times. We expect such extended measurements to be feasible using higher flux sources.

We have demonstrated that measurement of the near-edge structure of the energy dependence of the power diffracted by a CTR can be used to measure the oxidation state of atoms at an interface. We select Cr atoms by choosing the Cr K-absorption edge. We are sensitive only to Cr atoms at the buried interface because the Al_2O_3 substrate does not contain Cr atoms, and only the first three atomic layers of the Cr_2O_3 film are coherent with the substrate to a measurable extent. Analysis of the fine structure of the energy dependence of CTR diffraction is widely applicable. While this technique requires the truncation rods of a crystalline substrate, the film need not be crystalline, as the first layers of amorphous films have been found to be coherent with crystalline substrates.[2] As discussed by Stragier *et al.*,[16] measurement of the energy dependence of CTR's and other diffraction features provides a means of isolating particular sets of symmetry sites for spectroscopic measurements.

ACKNOWLEDGMENTS

We are grateful to P. R. Zschack and M. C. Nelson for assistance in beamline operation. We have benefitted from discussions with G. E. Ice and H. Yakel. This research was sponsored jointly by the U.S. Air Force Office of Scientific Research under interagency agreement DOE Grant No. 1854-A077-Al, USAF Grant No. AFOSR-ISSA-92-3, and by the Division of Materials Sciences, U.S. Department of Energy, under Contract No. DE-AC05-84OR21400 with Martin Marietta Energy Systems, Inc.; it was conducted in part at NSLS, which is supported by the U.S. Department of Energy under Contract No. DE-AC02-76CH00016.

*Also at Department of Material Science and Engineering, University of Tennessee, Knoxville, TN 37996.

[1]R. Feidenhans'l, Surf. Sci. Rep. **10**, 105 (1989).
[2]I. K. Robinson, W. K. Waskiewicz, R. T. Tung, and J. Bohr, Phys. Rev. Lett. **57**, 2714 (1986).
[3]I. K. Robinson, R. T. Tung, and R. Feidenhans'l, Phys. Rev. B **38**, 3632 (1988).
[4]E. D. Specht *et al.*, Phys. Rev. B **43**, 12 425 (1991).
[5]F. J. Walker, E. D. Specht, and R. A. McKee, Phys. Rev. Lett. **67**, 2818 (1991).
[6]H. Hong, R. D. Aburano, D.-S. Lin, H. Chen, T.-C. Chiang, P. Zschack, and E. D. Specht, Phys. Rev. Lett. **68**, 507 (1992).
[7]D. J. Tweet, K. Akimoto, T. Tatsumi, I. Hirosawa, J. Mizuki, and J. Matsui, Phys. Rev. Lett. **69**, 2236 (1992).
[8]S. R. Andrews and R. A. Cowley, J. Phys. C **18**, 6427 (1985).
[9]I. K. Robinson, Phys. Rev. B **33**, 3830 (1986).
[10]E. Fontes, Jr., K. W. Evans-Lutterodt, B. J. Hinch, E. Vlieg, I. K. Robinson, J. R. Patel, and L. H. Dubois (unpublished).
[11]G. Reiter and S. C. Moss, Phys. Rev. B **33**, 7209 (1986).
[12]*X-Ray Absorption: Principles, Applications, and Techniques of EXAFS, SEXAFS, and XANES,* edited by D. C. Koningsberger and R. Prins (Wiley, New York, 1988).
[13]B. E. Warren, *X-Ray Diffraction* (Dover, New York, 1990), pp. 10 and 28.
[14]P. Dreier, P. Rabe, W. Malzfeldt, and W. Niemann, J. Phys. C **17**, 3123 (1984).
[15]J. J. Hoyt, D. de Fontaine, and W. K. Warburton, J. Appl. Cryst. **17**, 344 (1984).
[16]H. Stragier, J. O. Cross, J. J. Rehr, L. B. Sorensen, C. E. Bouldin, and J. C. Woicik, Phys. Rev. Lett. **69**, 3064 (1992).
[17]L. A. Grunes, Phys. Rev. B **27**, 2111 (1983).
[18]J. E. Penner-Hahn, M. Benfatto, B. Hedman, T. Takahashi, S. Doniach, J. T. Groves, and K. O. Hodgson, Inorg. Chem. **25**, 2255 (1986).
[19]R. A. McKee, F. A. List, and F. J. Walker, in *Multilayers: Synthesis, Properties, and Nonelectronic Applications,* edited by T. W. Barbee, Jr., F. Spaepen, and L. Greer, MRS Symposia Proceedings No. 103 (Materials Research Society, Pittsburgh, 1988), p. 35.
[20]A. Habenschuss, G. E. Ice, C. J. Sparks, and R. A. Neiser,

Nucl. Instrum. Methods A **266**, 215 (1988).
[21]W. R. Busing and H. A. Levy, Acta Crystallogr. **22**, 457 (1966).
[22]E. D. Specht and F. J. Walker, J. Appl. Crystallogr. (to be published).
[23]M. M. Hall, Jr., V. G. Veeraraghavan, H. Rubin, and P. G. Winchell, J. Appl. Crystallogr. **10**, 66 (1977).
[24]P. Croce and L. Névot, Rev. Phys. Appl. **11**, 113 (1976).
[25]*International Tables for X-Ray Crystallography,* edited by C. H. MacGillavry and G. D. Rieck (Kynoch, Birmingham, England, 1962), Vol. III, p. 233.
[26]B. E. Warren, *X-Ray Diffraction* (Dover, New York, 1990), p. 326.
[27]R. W. G. Wyckoff, *Crystal Structures* (Interscience, New York, 1951).
[28]*International Tables for X-Ray Crystallography,* edited by J. A. Ibers and W. C. Hamilton (Kynoch, London, 1974), Vol. IV, p. 99.
[29]D. T. Cromer and D. Liberman, J. Chem. Phys. **53**, 1891 (1970).
[30]W. H. McMaster, N. K. Del Grande, J. H. Mallett, and J. H. Hubbell, *Compilation of X-Ray Cross Sections* (Lawrence Radiation Laboratory, Livermore, CA, 1969).
[31]H. Saafeld, Z. Kristallogr. Kristallgeom. Krystallphys. Kristallchem. **120**, 342 (1964).
[32]M. A. Blokhin, *Methods of X-Ray Spectroscopic Research* (Pergamon, Oxford, 1965), p. 342.
[33]G. E. Ice (private communication). The Kramers-Kronig transform is computed using the program PRIME written by G. E. Ice.